energies

MDPI

Article

Multi-Objective Hybrid Optimization for Optimal Sizing of a Hybrid Renewable Power System for Home Applications

Md. Arif Hossain [1,*], Ashik Ahmed [1], Shafiqur Rahman Tito [2], Razzaqul Ahshan [3,*], Taiyeb Hasan Sakib [4] and Sarvar Hussain Nengroo [5,*]

1 Department of Electrical and Electronic Engineering, Islamic University of Technology, Dhaka 1212, Bangladesh
2 Department of Software Engineering, University of Waikato, Hamilton 3216, New Zealand
3 Department of Electrical and Computer Engineering, College of Engineering, Sultan Qaboos University (SQU), Muscat 123, Oman
4 Department of Electrical and Electronic Engineering, Brac University, Dhaka 1212, Bangladesh
5 Cho Chun Shik Graduate School of Mobility, Korea Advanced Institute of Science and Technology (KAIST), 291, Daehak-ro, Yuseong-gu, Daejeon 34141, Republic of Korea
* Correspondence: arifhossain@iut-dhaka.edu (M.A.H.); razzaqul@squ.edu.om (R.A.); sarvar@kaist.ac.kr (S.H.N.)

Abstract: An optimal energy mix of various renewable energy sources and storage devices is critical for a profitable and reliable hybrid microgrid system. This work proposes a hybrid optimization method to assess the optimal energy mix of wind, photovoltaic, and battery for a hybrid system development. This study considers the hybridization of a Non-dominant Sorting Genetic Algorithm II (NSGA II) and the Grey Wolf Optimizer (GWO). The objective function was formulated to simultaneously minimize the total energy cost and loss of power supply probability. A comparative study among the proposed hybrid optimization method, Non-dominant Sorting Genetic Algorithm II, and multi-objective Particle Swarm Optimization (PSO) was performed to examine the efficiency of the proposed optimization method. The analysis shows that the applied hybrid optimization method performs better than other multi-objective optimization algorithms alone in terms of convergence speed, reaching global minima, lower mean (for minimization objective), and a higher standard deviation. The analysis also reveals that by relaxing the loss of power supply probability from 0% to 4.7%, an additional cost reduction of approximately 12.12% can be achieved. The proposed method can provide improved flexibility to the stakeholders to select the optimum combination of generation mix from the offered solutions.

Keywords: battery; hybrid renewable energy system (HRES); genetic algorithm (NSGA) II; grey wolf optimizer (GWO); non-dominant sorting; optimization; photovoltaics; wind energy

Citation: Hossain, M.A.; Ahmed, A.; Tito, S.R.; Ahshan, R.; Sakib, T.H.; Nengroo, S.H. Multi-Objective Hybrid Optimization for Optimal Sizing of a Hybrid Renewable Power System for Home Applications. *Energies* **2023**, *16*, 96. https://doi.org/10.3390/en16010096

Academic Editor: Antonio Cano-Ortega

Received: 25 November 2022
Revised: 17 December 2022
Accepted: 19 December 2022
Published: 21 December 2022

1. Introduction

1.1. General and Motivation

Since the twenty-first century, the world has seen a rapid acceleration in electrical energy consumption. Due to the continuous increase in consumption, the energy demand is predicted to rise by about 53% by 2035 [1]. Fossil fuel resources are gradually diminishing to meet the ever-increasing energy demand. As such, renewable energy sources, an alternative to fossil fuel, have been steadily increasing over the past years. Besides, renewable energy sources are also environment-friendly and freely available [2]. The scarcity of conventional resources has motivated modern-day researchers to tap into renewable alternatives. A recent hike in fuel prices in energy sector also heightened the interest of the scientific community to explore the full potential of renewable resources. The recent global pandemic has also sped up the energy sector's transition to sustainable solutions.

However, the unpredictable nature of their output makes them expensive and unreliable, which necessitates the use of more than one source of energy to complement each other. Such a system is known as Hybrid Renewable Energy System (HRES). A stand-alone HRES provides many reliable outcomes compared to a single source-based system in terms of cost and efficiency [3]. HRES is gaining popularity, especially in remote areas, due to the price rise of petroleum products [4]. A significant amount of research has been carried out related to HRES for cost-effective and efficient deployment of such systems for islanded locations.

Auckland, New Zealand, currently depends largely on the other parts of the country for electricity generation and the current growth in energy demand is reported to result in discrepancies in future energy usage [5]. The government of New Zealand has already taken initiatives to promote decentralized sustainable energy solutions [6]. To implement appropriate HRES to take care of the future energy demand in Auckland, proper analysis is required for efficient and economically viable solutions.

1.2. Literature Review

In the literature, hybrid systems with various configurations were economically assessed for various contexts. Authors in [7] proved that a hybrid system with energy storage is more economical than a system without energy storage [8,9]. Besides, energy storage devices add flexibility, minimize intermittences, and provide backup generation, making a renewable generation system more attractive [10]. A photovoltaic (PV), wind turbine (WT), and energy storage-based hybrid system were proposed for a cement factory in Jordan.

Authors in [11] used WT, PV, and fuel cell (FC) generation systems to satisfy the load of a typical home in the Pacific Northwest. This system used a hydrogen storage tank as the energy storage system. The high initial cost of the required hydrogen tank for FC makes the system expensive [12]. Research in [13] proved that PV, WT, and battery systems are the most economical and environment-friendly combinations for HRES. Authors in [14] have proven, using seven different optimization techniques, that a hybrid PV–WT–battery system is the most cost-effective combination for outlying areas compared to a PV–battery, a WT–battery, and a PV–WT configuration. A comparative analysis was carried in terms of HRES research focus and technical tools used for assessment in study [15]. In [16], different architectures were taken into consideration for optimal sizing of HRES components for a specific location in Bangladesh with practical load data. The result concluded PV–WT with biogas to be the most effective for the considered location.

The sizing of an HRES is highly complex due to the randomness of energy generation from these renewable sources. While an oversized HRES can quickly satisfy the load demand, it is unnecessarily expensive. In contrast, an undersized HRES is economical but often fails to satisfy the load demand reliably. Thus, optimum sizing of an HRES is expected, which necessitates the development of the mathematical model of the system components [17]. In this regard, authors in [18] performed optimal sizing of a stand-alone hybrid PV/wind/hydrogen system for supplying a desalination unit using an iterative optimization technique. The algorithm considers all the possible configurations that can satisfy the freshwater requirements of the consumers. The study, however, needs to consider the components' associated maintenance cost, and evaluating all the possible configurations is often time-consuming for most modern-day complex problems. Since classical techniques are not efficient in solving complex optimization problems [19], modern techniques and software tools are available alternatives. HOMER, iHOGA, and TRNSYS have been extensively used among the software tools. For the economic and technical analysis of a stand-alone HRES consisting of PV, wind, diesel generator, and batteries, HOMER software has been used [20], and the configuration was evaluated for a large resort in Malaysia. The authors also used HOMER in [21] for optimizing a hybrid wind/PV/battery system for a household in Urumqi, China. An HRES composed of a PV–WT battery with a diesel generator was considered for optimal sizing using a non-dominated sorting genetic algorithm for a rural location in Bangladesh [22]. This study also used HOMER as the preferred

software tool. A solar–wind–fuel cell hybrid system was studied for a remote area using HOMER [23]. Using the same software tool, economic analysis of a renewable mix hybrid system for a diesel community on an island in Oman is investigated in [24].

Authors in [25] used a deterministic approach for sizing a PV–wind-based hybrid system and the software used was TRNSYS. The study also carried out a comparison between two size deterministic methods namely yearly average month (YAM) and worst month (WM) methods. In another study [26], a detailed comparison of the PV–wind–battery system configuration with the PV–wind, PV–battery, and wind–battery sub-configurations was presented. The study evaluated the energy performance of the system components on an hourly basis and implemented it in the TRNSYS 17 environment. In [27], the authors proposed a novel energy reliability constrained (ERC) method to a grid-connected hybrid system. A detailed comparison between the proposed ERC and pareto front multi-objective optimization was also shown. This system was also simulated in TRNSYS 17 environment. However, according to [28], though software tools can be extensively used for sizing and technical and economic studies, they still need to be made more flexible for increased usage in control and stability related studies. Authors in [29] demonstrated that intelligent techniques such as PSO performs better than well-established software tools such as HOMER. Besides, the sizing of various HRES configurations using software tools is based on some assumptions and sequences [30]. In a detailed review study on size optimization methodologies, authors in [19] concluded that artificial and hybrid algorithms, which are termed as modern techniques, generate more precise optimization results than software tools since the hybrid algorithms often have the capability of solving multi-objective optimization problems. In this context, a hybrid PSO with small population size termed as HPSO-SP was proposed in [31] for solving the optimal short term hydro-thermal unit commitment problem.

Among the evolutionary optimization algorithms, genetic algorithm (GA) has proven to be the most effective. GA was used in [32] for minimizing the cost function of a PV/WG system, which ensured complete fulfilment of load energy requirements for a full period of 20 years. Nature-inspired algorithms like particle swarm optimization (PSO) were also used by authors in [33] for reducing the Levelized Cost of Energy (LCE). More recently in 2019, grasshopper optimization algorithm (GOA) was employed in [34] for determining the optimum configuration of an HRES consisting of PV modules, WT, battery, and diesel generator. The objective of this study was to obtain a lower cost of energy (COE). The authors also presented a comparison of the applied GOA with PSO and cuckoo search (CS) algorithm. However, in all these studies, the authors opted for single-objective optimization (SOO) rather than multi-objective optimization (MOO). Studies in [35] show that MOO provides better flexibility to the designers in selecting the most optimal solution. In this aspect, MOO has been carried out by authors in [36] where both annual cost system (ACS) and loss of power supply probability (LPSP) were minimized applying multi-objective genetic algorithm. In 2015, Azadeh et al. in [37] employed non dominated sorting algorithm-II (NSGA-II) to achieve minimum system cost and maximum reliability. NSGA-II was also employed in [38] to find an optimal configuration of a system consisting of a WT, FC, alkaline electrolyzer, battery, and a supercapacitor bank for an off-grid application. The main aim of this study was to simultaneously minimize total annual cost (TAC) and LPSP. However, the proposed model is only applicable for places with high wind speed, and besides, the need for FC also makes the system expensive. Recently, authors in [39] applied hybrid GA-PSO for SOO and multi-objective PSO (MOPSO) for MOO in order to minimize the total present cost and loss of load expected (LOLE). In the study in [40], Ref [41] adapted the GWO algorithm for optimal sizing of hybrid systems.

1.3. Research Gap and Contributions

It is evident from the review of literature that single objective optimization techniques were analyzed in-depth for the optimal sizing of HRES. In comparison, fewer studies were focused on the analysis and sizing of HRES as multi-objective optimization. Despite the fact

that numerous research favored combining different algorithms, appropriate justification for the hybridization of algorithms was limited. NSGA-II and GWO were independently applied for optimal HRES configurations in different studies. NSGA-II has the characteristics of fast and efficient convergence, albeit with computational complexity. On the other hand, GWO is simpler in computation but has a slower convergence speed. Hence, hybridization of GWO with NSGA-II is expected to provide reduced computational burden along with satisfactory speed and efficiency. Despite having a strong potential for renewable energy, there is little literature available on Auckland, New Zealand's HRES analysis.

In this study, an optimal energy mix hybrid power system was designed for a residential home in Auckland, New Zealand. The design process employs two objective functions: minimizing the total cost and loss of power supply probability (LPSP). Since hybrid algorithms provide the most precise optimum results for the sizing approach, a hybrid multi-objective optimization algorithm combining NSGA-II [42] and GWO [43] was employed. Such a combination of these techniques can improve the exploitation and exploration capability of NSGA-II. The performance of this hybrid optimization technique was analyzed and compared with other well-established MOO algorithms, such as MOPSO and NSGA-II, to justify the overall performance improvements of the hybrid algorithm. The main contributions of this work are as follows:

- To the authors' best knowledge, this is the only contribution to propose an optimal mix of HRES using hybrid optimization technique as multi-objective optimization for a typical residential load in Auckland, New Zealand.
- Performance testing of the proposed optimization algorithm to justify the efficacy in designing HRES and comparing against other MOO algorithms, such as MOPSO and NSGA-II, in the literature.
- Generating multiple solutions with varying levels of LPSP to provide flexibility in choice of HRES deployment for the policy makers and energy service providers of Auckland, New Zealand.
- Statistical justification of the proposed hybridization of algorithms is provided.

1.4. Paper Structure

The rest of the paper is arranged as follows: the methodology is explained in Section 2. Section 3 presents results and discussion on this study, and finally the paper is concluded in Section 4.

2. Methodology

This section describes the methodology for determining the optimal configurations of an HRES as follows: (i) System modelling; (ii) Demand, weather data, wind turbine, PV module, and battery specification; (iii) The mathematical modelling of a wind turbine, PV, and battery; and (vi) Objective function formulation. Finally, the hybrid optimization algorithm is explained in detail. It is important to note that all calculations are done on an hourly basis. The proposed optimization algorithm simultaneously minimizes both LPSP and the total life cycle cost of the HRES.

2.1. Hybrid Renewable System Components

Figure 1 illustrates the proposed HRES for meeting the load demand of a home. It consists of PV, WT, DC-AC converters, DC-DC converters, battery storage, and DC and AC loads [44]. The DC load is directly connected to the DC bus, and the AC load receives power through the DC-AC inverter.

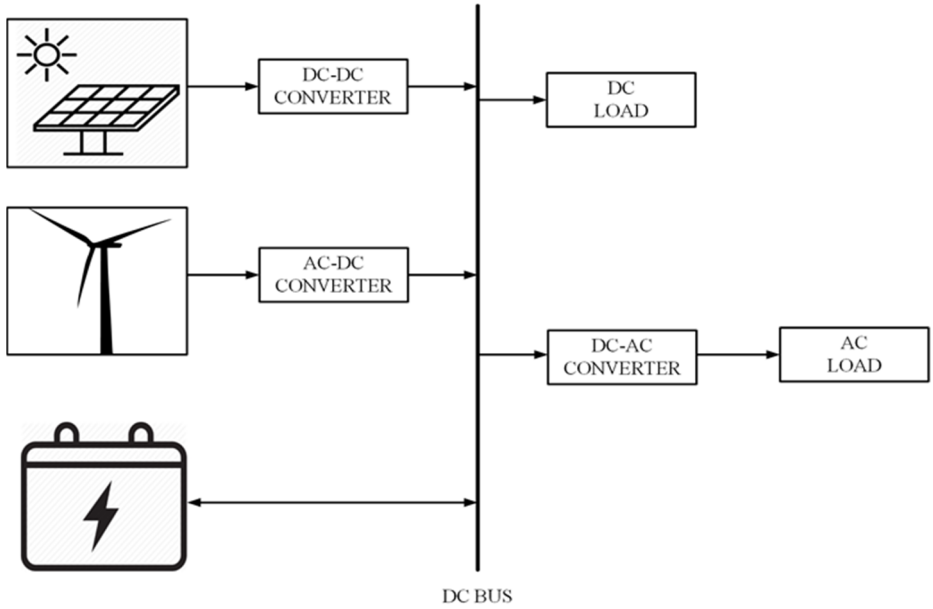

Figure 1. Renewable mix hybrid power generation system.

2.2. Load Demand

Figure 2 presents one-day hourly load data for a typical home during summer in Auckland, New Zealand [45]. The peak power demand is about 2 kW and the lowest power demand is about 0.75 kW. The daily average load demand is 1191.08 W.

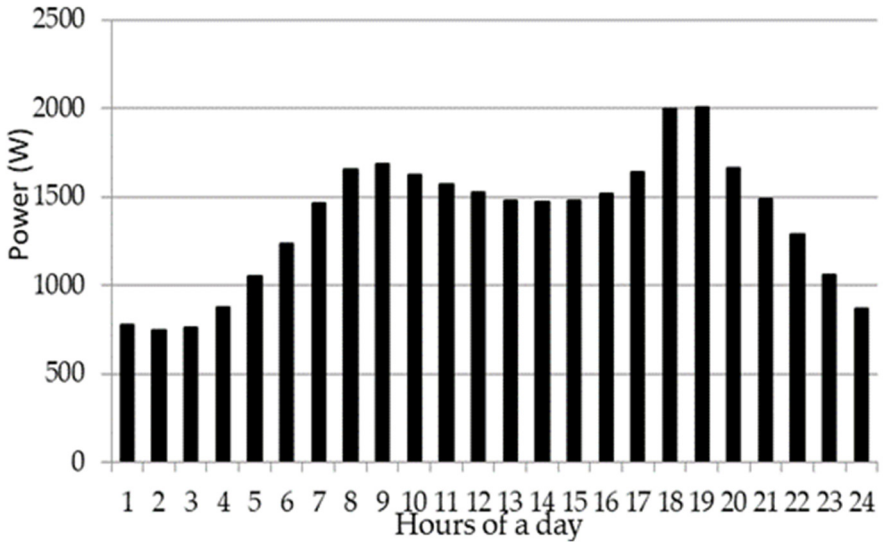

Figure 2. Hourly load demand for a home in a day during summer.

2.3. Renewable Resources

Hourly wind speed in m/s and global horizontal radiation in Wh/m^2 for a year are considered in this study, and are depicted in Figure 3. The annual average wind speed is 4.80 m/s at the anemometer height. The annual average solar irradiation is 171.28 Wh/m^2 [46]. The wind speed is consistent over the year; however, the solar irradiation is low during the winter.

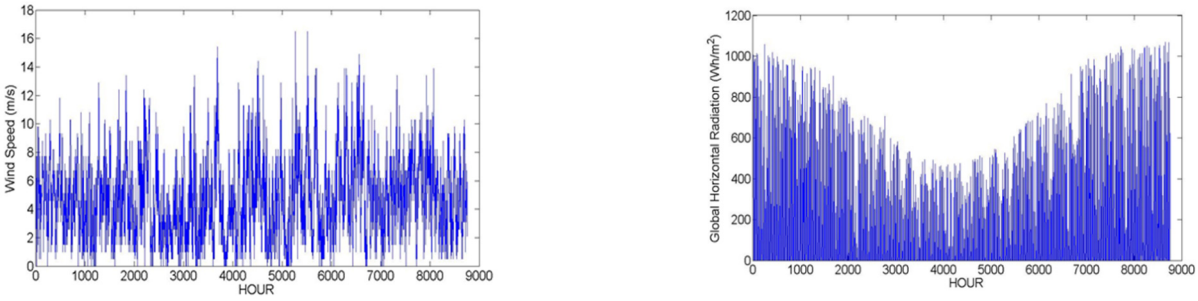

(**a**) (**b**)

Figure 3. Weather data considered—(**a**) hourly wind speed data for a year, (**b**) hourly irradiance data for a year.

2.4. Mathematical Modeling of the System Components

There are two sources of energy in the adopted HRES and an energy storage device. The mathematical modelling of all these components is interpreted below.

2.4.1. Wind Turbine

Based on the study by [47], the specific power output, P_w (W/m^2), depends on the wind speed of that particular site and is expressed by

$$\begin{aligned} P_w(t) &= 0 \quad v(t) < v_{ci} \\ P_w(t) &= av^3(t) - bP_r \quad v_{ci} \le v(t) < v_r \\ P_w(t) &= P_r \quad v_r \le v(t) < v_{co} \\ P_w(t) &= 0 \quad v(t) \ge v_{co} \end{aligned} \tag{1}$$

From Equation (1), it is observed that whenever the wind speed, $v(t)$, is less than some critical value which is known as cut in speed, v_{ci}, or higher than some critical value, defined as cut out speed, v_{co}, the output power from the wind turbine is zero. Rated power, P_r is given by the WT when the wind speed is in between rated speed, v_r, and v_{co}. When the wind speed is greater than v_{ci} and less than v_r, power obtained from a nonlinear relationship combining $v(t)$ and P_r.

Here, $a = \frac{P_r}{v_r^3 - v_{ci}^3}$, $b = \frac{v_{ci}^3}{v_r^3 - v_{ci}^3}$ are constants which are defined from the manufacturer's end. The cut in, rated, and cut out speed of the wind turbine can be found from the manufacturer of the selected turbine [44]. The wind speed at any height is obtained from the following equation [48].

$$v = v_r \left(\frac{h}{h_r} \right)^{\alpha} \tag{2}$$

In Equation (2), v_r and v are the wind speed at the reference height and hub height, respectively, α is the power law coefficient, taken as $1/7$ for open space [49], h is the WG installation height, and h_r is the reference height. As the value of α is $1/7$, v and h are nonlinearly related. It is to be noted that the reference height is considered to be 33 m and the hourly wind speed at the reference height is obtained from typical meteorological year (TMY) data. Therefore, the electrical power as obtained as output from a WG can be found by

$$P_{WG} = P_w A_{WG} \eta_{wG} \tag{3}$$

where P_{WG} is the power produced by the WGs, A_{WG} is the total swept area of a WG, and η_{wG} is the efficiency of WG and the corresponding converters. Table 1 presents the specification of the wind turbine used in this study.

Table 1. Specification of the WG.

Power (W)	h_{low} (m)	h_{high} (m)	WG Capital Cost ($)	Tower Capital Cost ($/Unit Length)
1000	11	35	2400	55

2.4.2. Solar Photovoltaic Module

The output power from a PV array is dependent on the solar radiation incident on the PV surfaces and other related parameters specified by the manufacturer. The expression used to calculate the output power is given by [32,50].

$$P_{PV}(t,\beta) = N_S \cdot N_P \cdot V_{OC}(t,\beta) \cdot I_{SC}(t,\beta) \cdot FF(t) \quad (4A)$$

$$V_{OC}(t,\beta) = \{V_{OC-STC} - K_V T_C(t)\} \quad (4B)$$

$$I_{SC}(t,\beta) = \{I_{SC-STC} + K_I[T_C(t) - 25\,^{\circ}C]\}\frac{G(t,\beta)}{1000} \quad (4C)$$

$$T_C(t) = T_A + (NCOT - 20\,^{\circ}C)\frac{G(t,\beta)}{800} \quad (4D)$$

In Equation (4A), P_{PV} is the power produced by PV modules, t is a particular time (hour in this study), β is the tilt angle of the PV modules, and N_S and N_P are the number of PV modules connected in series and parallel, respectively, in an array. V_{OC} and I_{SC} represent the open circuit voltage and short circuit current of a PV module respectively, FF is the fill factor, the ratio of the product of V_{Max} and I_{Max} to the product of V_{OC} and I_{SC}. In Equation (4B), V_{OC} and V_{OC-STC}, which are open circuit voltage for standard test conditions, are equal if the cell is operated at ambient temperature, but if the temperature is different, due to K_I, V_{OC} will be different. I_{SC} is calculated by Equation (4C) and depends on K_I and G where K_V and K_I are the open circuit voltage temperature coefficient and short circuit current temperature coefficient, respectively, and G represents the global solar irradiance on a PV module, which depends on time of the day and tilt angle of the solar cell. In Equation (4D), T_A is the ambient temperature and $NCOT$ is the nominal operating cell temperature, operating temperature, and $Tc(t)$ is calculated from this relation.

Thus, incorporating efficiency, the total output power from a PV array, having N_S PV modules in series and N_P PV modules in parallel, follows the following expression

$$P_{amray}(t,\beta) = \eta_{PV} N_S N_P P_{PV}(t,\beta) \quad (5)$$

where η_{PV} is the PV–module's and related converter's efficiency [42]. It is important to note that the numbers of PV modules in series is readily determined by the magnitude of the DC bus voltage, whereas the numbers of parallel PV modules are obtained from the optimization algorithm. Table 2 presents PV module data used in this study.

Table 2. Specification of the PV module.

V_{OC-STC} (V)	I_{SC-STC} (A)	V_{max} (V)	I_{max} (A)	P_{max} (W)	Capital Cost ($)	$NCOT$ (°C)
64.8	6.24	54.7	5.86	320	640	45

2.4.3. Battery

An energy storage device is an essential part of any HRES. Because it is a widespread phenomenon, energy generated will rarely equal the energy demand at every hour of the day. Thus, storing surplus energy when energy generation is more than the demand becomes necessary. On the contrary, supplying the deficit energy from the energy storage device when the energy demand exceeds the generation.

In this study, the chosen battery is of lead-acid type. The factor that determines the charging and discharging state of the battery is known as instantaneous state of charge (SOC) and it follows the following equation [51].

$$\mathrm{SOC}(t) = \mathrm{SOC}(t-1) \cdot \left(1 - \frac{\sigma \cdot \Delta t}{24}\right) + \frac{I_{bat}(t) \cdot \Delta t \cdot \eta_{bat}}{C_{bat}} \tag{6}$$

It is observed from Equation (6) that for SOC at any hour, t is a function of previous state of charge $\mathrm{SOC}(t-1)$. Here, σ is the self-discharge rate of a battery which signifies self-running electrochemical processes which cause batteries to discharge more or less quickly, even if no electrical consumers are connected. The self-discharge rate of a battery is taken to be 0.2% per day for this study [52], $I_{bat}(t)$ is the battery current at t-th hour measured in ampere, C_{bat} (Ah) is the nominal capacity of a battery, η_{bat} is the battery charging/discharging efficiency, and Δt is the hourly time step. However, the efficiency of the battery is different for different states of charge, and it is taken to be 1 while discharging and 0.8 while charging [43]. Therefore, the current obtained from the battery due to its incorporation with PV and WG is given by the equation, as shown in (7).

$$I_{bct}(t) = \frac{P_{PV}(t) + P_{WG}(t) - P_{\mathrm{Load}}(t)}{V_{bct}} \tag{7}$$

where V_{bct} is the nominal voltage of each individual battery, P_{PV} and P_{WG} are calculated from Equations (1) and (4A), respectively. Table 3 presents the battery specification in this study.

Table 3. Specification of the battery model.

Price ($)	V_{bat}(V)	Capacity (A h)
1239	12	357

2.5. Problem Formulation for Optimization

There is a probability that the proposed hybrid model may sometimes be unable to satisfy the load demand in order to be economically viable; such probability is defined as loss of power supply probability (LPSP) [53]. For maximizing quality and minimizing cost, this study aims at simultaneously minimizing both LPSP and the total cost over the life of the HRES. The objective function includes capital costs comprising of the initial costs of PVs, WGs, batteries, along with 20 years of total maintenance and operation cost, and is defined by Equation (8) [32].

$$\text{Minimize } f(N_{PV}, N_{WG}, N_{bat}, \beta, h) = \left[\begin{array}{l} N_{PV}(C_{PV} + 20M_{PV}) + \\ N_{WG}(C_{WG} + 20M_{WG} + h \cdot C_h + 20hM_h) + \\ N_{bat}(C_{bat} + y_{bat}C_{bat}) + (20 - y_{bat} - 1)M_{bat}] \end{array}\right. \tag{8}$$

subject to the constraints

$$\begin{array}{l} N_{WG} \geq 0, \\ N_{PV} \geq 0, \\ N_{bat} \geq 0, \\ 90^\circ \geq \beta \geq 0, \\ 11 > h > 40. \end{array} \tag{9}$$

In Equation (8), N_{PV}, N_{WG}, and N_{bat} are the number of PV modules, WGs, and batteries, respectively, C_{PV}, C_{WG}, and C_{bat} are the capital cost of a PV module, WG, and battery, respectively, M_{PV}, $20M_{WG}$, and M_{bat} are the annual maintenance cost of a PV module, WG and battery, respectively, C_h is the capital cost per unit height of WG tower, M_h is the yearly maintenance cost per unit height of a WG tower, and y_{bat} is the expected number of battery replacements in a period of 20 years [44].

In the applied optimization method, two optimization methods were incorporated to create a hybrid optimization algorithm, which is depicted in Figure 4. The hybrid algorithm commences with the normal initialization of NSGA II [42]. NSGA II is a MOO aiming to generate a set of optimal solutions in contrast to a single solution as in SOO. The set of optimal solutions is known as a pareto-optimal solution, and NSGA II is well known for generating the pareto-optimal solution [54]. None of the solutions in the pareto-optimal set can be termed as dominating the others concerning the given objective functions. This decision solely lies in the designer's perspective and provides much flexibility in determining the best solution from the pareto-optimal set based on the specific requirements/conditions. It is seen from Figure 4 that a random population of P_primary is created, and it is a set of the population consisting of the random population P_primary is rectified if any randomly generated parameters go beyond the specified constraints in Equation (9). This population is sorted based on non-domination and crowding distance operator, and the new population is termed P_primary_sorted. However, before accessing the core part of the NSGA algorithm, which is cross-over and mutation, the population termed P_primary_sorted was fed to another algorithm known as GWO [43].

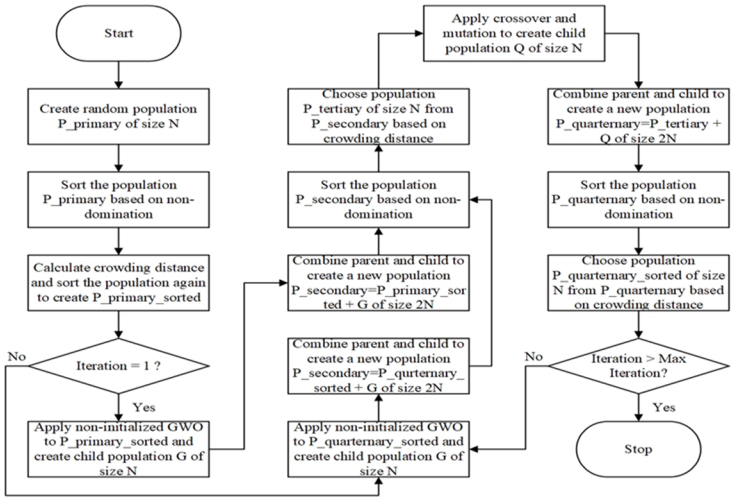

Figure 4. Implementation steps of hybrid (NSGA-GWO) multi-objective optimization algorithm for optimal sizing of a hybrid renewable energy system.

GWO promises a high local optima avoidance probability and better exploration ability. It is to be noted that the GWO is declared to be non-initialized because instead of generating a random population in GWO, the P_primary_sorted population obtained from the initial population set of NSGA II is taken to be the initial population of GWO. Although GWO is an SOO, it produces child population G of the same size as the parent population. This is because GWO updates the positions of all the search agents and sorts them based on the fitness value in each iteration. Therefore, the first member in the sorted search agents is declared the best search agent in each iteration and the process is continued for the defined number of iterations. In the hybrid algorithm, instead of taking the best search agent, the whole pack of search agents is considered the child population, and obviously, the first member remains the best search agent. Thus, the size of child population G remains equal to that of the parent population. This child population G, as obtained from GWO, is added with P_primary_sorted (when iteration = 1) or P_quarternary sorted (when iteration > 1) to create a new population named P_secondary. P_secondary is now sorted again based on the non-domination and crowding distance operator to obtain the P_tertiary population on which the crossover and mutation occur, producing a child population Q. The rest of the algorithm is similar to NSGA II. Finally, P_quarternary was generated through a similar sorting operation, to produce the population P_quarternary_sorted. Provided the algorithm reaches the maximum number of iterations, it stops; otherwise, the algorithm

continues, as depicted in Figure 4. Therefore, the hybrid algorithm preserves the ingenuity of both algorithms and combines them to generate a much more reliable outcome.

3. Results and Discussion

The hybrid optimization algorithm discussed earlier was applied for a home load profile in Auckland, New Zealand. One-year (8760 h) hourly load data were utilized in this optimization process. Overall, 30 independent runs of the hybrid algorithm were recorded, each consisting of 100 iterations. The population size was set to 50. The simulation was carried out using a MATLAB/Simulink software tool [55], version R2018a, in a personal computer with an Intel core i5 processor and 8 GB RAM. It is important to note that the complete optimization problem was solved using the author's developed coding. In the present study, the optimum result of the total system cost was obtained while maintaining an LPSP of zero. It is because modern research should focus on assuring the best quality and thrive on finding the minimal cost for ensuring that quality. However, considering the cost constraints, this study also focuses on the cost obtained by increasing LPSP from zero to one. In order to ensure the viability of the hybrid algorithm, NSGA-II and MOPSO are also applied to the same load profile, and a comparative study was carried out. The three algorithms' optimum values obtained for each independent run were recorded and analyzed using Statistical Package for Social Sciences (SPSS) [56].

3.1. Statistical Descriptive Performance Comparison

Figure 5 illustrates the descriptive results of the proposed hybrid (NSGA-GWO), NSGA-II, and GWO optimization techniques. The mean value obtained from the hybrid algorithm is 33,871.11$, and that of the NSGA-II is 33,948.51$. Although the mean values obtained by these algorithms are fairly similar, for MOPSO, the cost rises to 69,637.78$. However, the mean value signifies the acceptability of an algorithm. For minimizing problems, the lower the mean, the better the acceptability, and vice versa. Besides the mean, further analysis is necessary to evaluate the overall prospect of an algorithm. The table shows that a minimum value of $32,797.48 was recorded from the hybrid algorithm, where NSGA-II obtained a slightly higher cost of $33,139.64 and MOPSO obtained a higher cost of $36,512.70. These results confirm that the optimum value achieved by the hybrid algorithm has a high probability of being the global minima and is not stuck at some local minima because the other two algorithms also reached a similar (though slightly higher) value. Variance measures how far a data set is spread out. The hybrid algorithm has a higher variance than NSGA-II, signifying that the data obtained from the hybrid algorithm are more spread out than NSGA-II. Both standard deviation and mean also support this conclusion since standard deviation measures how far the data are spread out from the mean value, and the median gives the middle value of the data set. Table 4 shows that the median and standard deviation are higher for the hybrid algorithm. It is to be noted that the variance, median, and standard deviation are not compared with MOPSO because the results obtained from MOPSO are not at all competitive with the other algorithms for this specific case.

It can be clearly seen that the solutions converge very quickly and attain the pareto-optimal solution. At the same time, NSGA-II requires more iterations to reach this pareto-optimal front. In NSGA-II, the solutions are initially scattered, gradually converging to form the pareto-optimal front. The gradual convergence of NSGA-II is also illustrated in Figure 6.

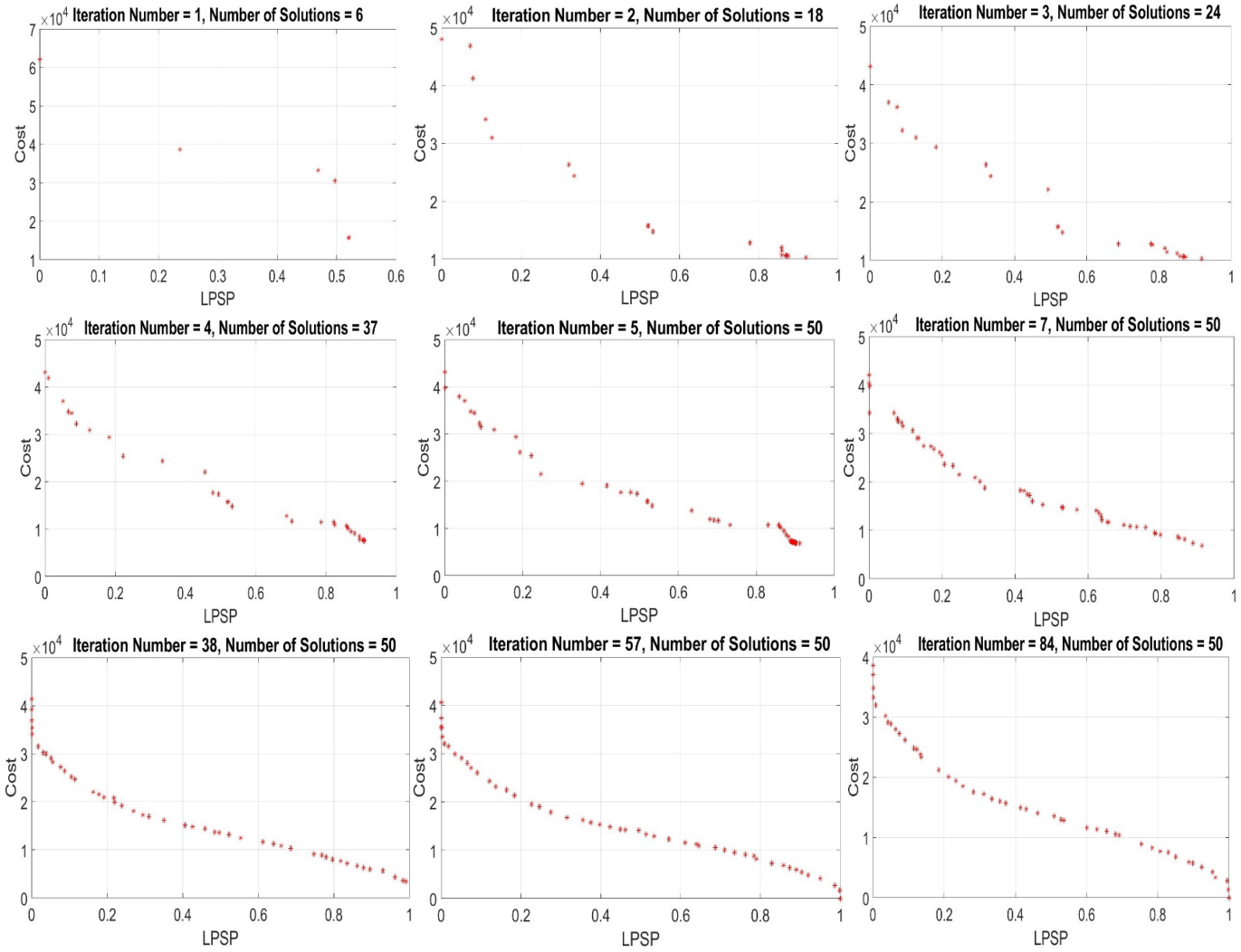

Figure 5. Gradual convergence of the solutions in the NSGA-GWO algorithm.

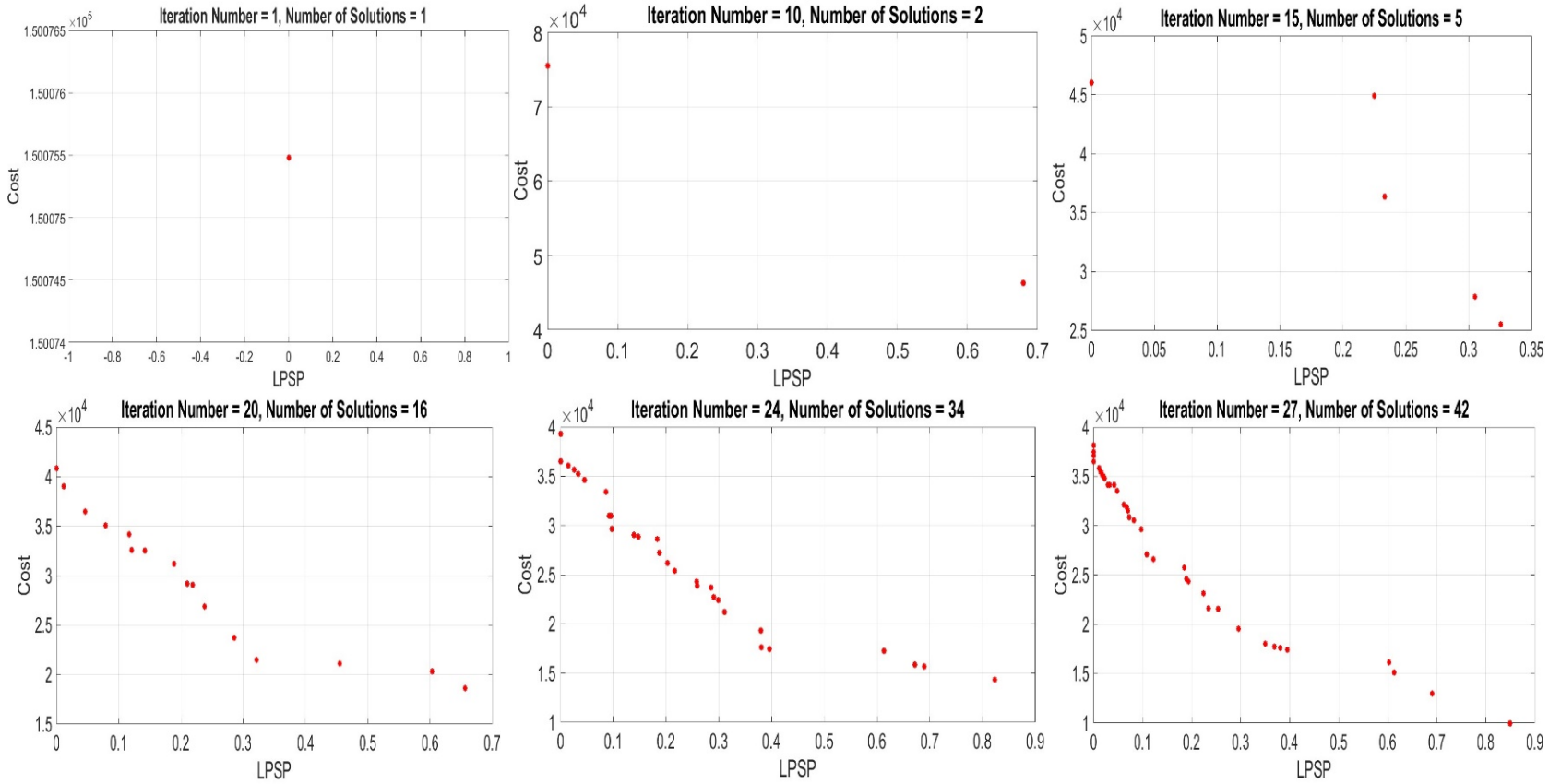

Figure 6. *Cont*.

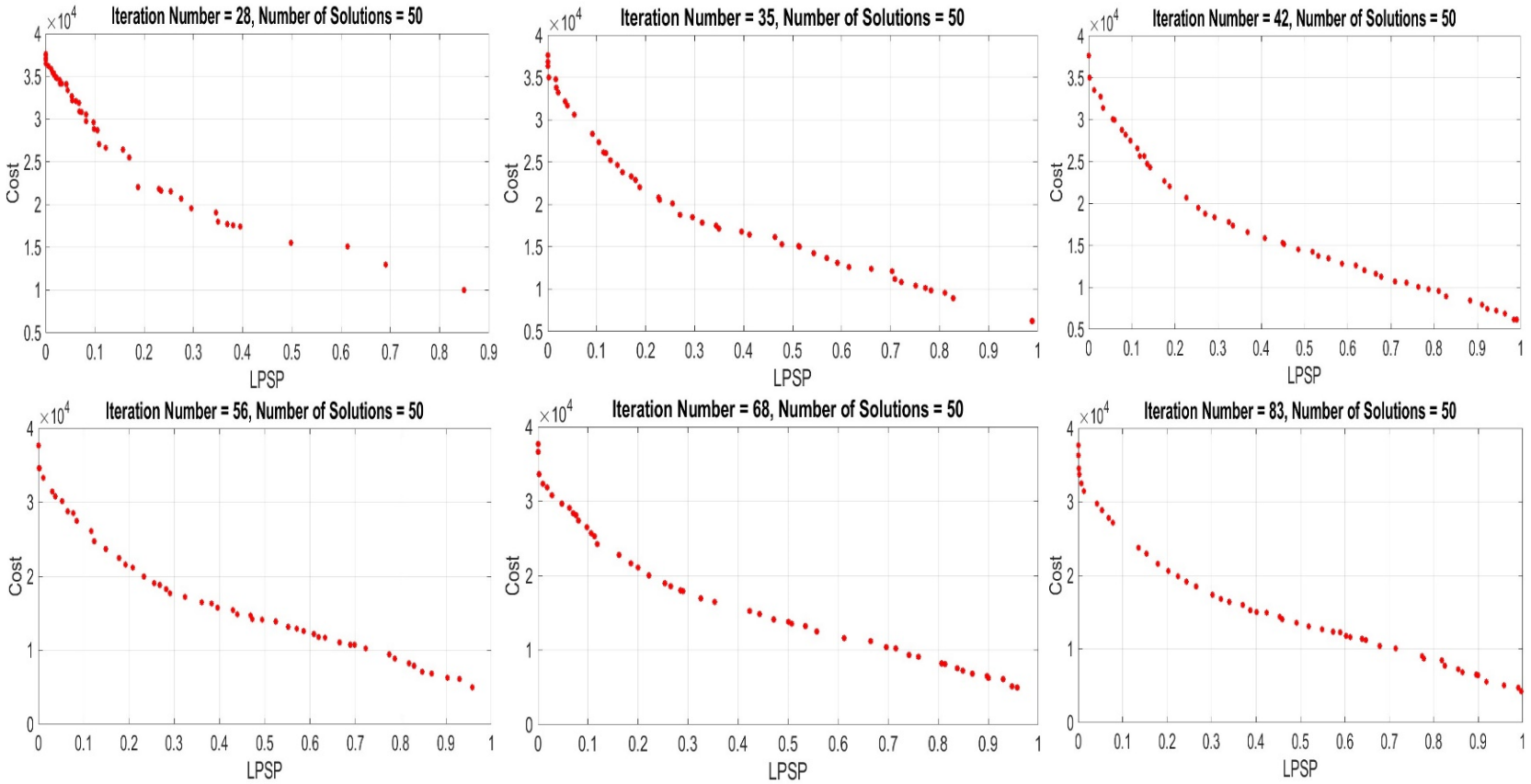

Figure 6. Gradual convergence of the solutions in NSGA-II.

Table 4. Statistical descriptive.

	NSGA-GWO Algorithm		NSGA II		MOPSO	
	Statistic	**Std. Error**	**Statistic**	**Std. Error**	**Statistic**	**Std. Error**
Mean	33,871.11	116.4525	33,948.51	102.2213	69,637.78	5071.5462
Median	33,812.78		33,785.08		67,215.25	
Variance	406,835.86		313,475.80		771,617,454.3	
Std. deviation	637.8368		559.8891		27,778.00	
Minimum	32,797.48		33,139.64		36,512.70	
Maximum	35,261.47		34,929.67		127,670.09	

3.2. Performance Comparison of Normality Test for the Hybrid, NSGA II, and MOPSO Algorithms

The normality tests of all three algorithms were carried out using Statistical Package for the Social Sciences (SPSS) and the results are shown in Table 5. This test gives an insight into how the data set is distributed. The null hypothesis states that the data are not statistically significantly different from the normal distribution. If the value of asymptotic sigma (Sig.) is less than 0.05, then the null hypothesis is rejected. Otherwise, it is accepted.

Table 5. Normality test data.

	Kolmogorov–Smirnov (K–S)			Shapiro–Wilk (S–W)		
	Statistic	**Degree of Freedom**	**Sig.**	**Statistic**	**Degree of Freedom**	**Sig.**
NSGA-GWO Algorithm	0.116	30	0.200	0.960	30	0.315
NSGA II	0.170	30	0.026	0.907	30	0.012
MOPSO	0.174	30	0.021	0.892	30	0.005

Table 5 reveals that the asymptotic sigma value of the hybrid algorithm in both tests is greater than 0.05, and for the other algorithms, it is less than 0.05. It confirms that the data (optimum costs) obtained from the hybrid algorithm are not statistically significant from the normal distribution. In contrast, the data recorded from the other two algorithms do not represent a normal distribution. With the normal distribution of data, the hybrid algorithm's standard deviation, variance, and median are higher than NSGA II (Table 4). Thus, the hybrid algorithm explores a more extensive area and gives the designer a more comprehensive range of options.

3.3. Comparative Study: Gradual Convergence towards Pareto-Optimal Front

Every optimization algorithm ultimately reaches a pareto front where the number of solutions in the set equals the initial population. The hybrid algorithm and NSGA-II reached the pareto-optimal front, where the number of solutions equals the initial population. However, MOPSO, even in 100 iterations, could not reach a pareto front where the number of solutions is equal to the initial population. The gradual convergence of the hybrid algorithm is depicted in Figure 5.

Figure 7 shows the number of iterations required to reach the pareto-optimal front for both NSGA-II and the hybrid algorithm. It can be seen that the minimum number of iterations required by NSGA-II to reach the optimal front is 12 and that for the hybrid algorithm is 2. It can be explained by the fact that a random population is fed to NSGA-II for cross-over and mutation. However, the updated and sorted population attained from the GWO was fed for cross-over and mutation in the hybrid algorithm. For this reason, the number of iterations required to reach the optimal front reduces significantly. It is evident from the above analysis that the hybrid algorithm not only has a high probability of ensuring global optimum results but also provides a better outcome than both NSGA-II and MOPSO in the field of HRES.

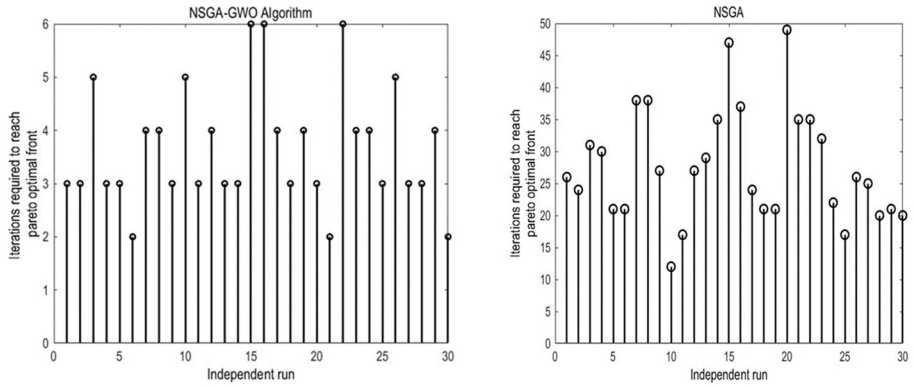

(a) (b)

Figure 7. (**a**) Number of iterations required in each independent run to reach the pareto-optimal front employing NSGA-GWO algorithm. (**b**) Number of iterations required in each independent run to reach the pareto-optimal front employing NSGA II.

3.4. Final Set of Solutions

Figure 8a,b explain the system cost variations with a varying LPSP. It can be observed from the figures that the cost reduces significantly once the LPSP is allowed to escalate. Thus, the decision now solely rests with the designer/company to choose the optimum result based on the requirements and ability of the designer/company.

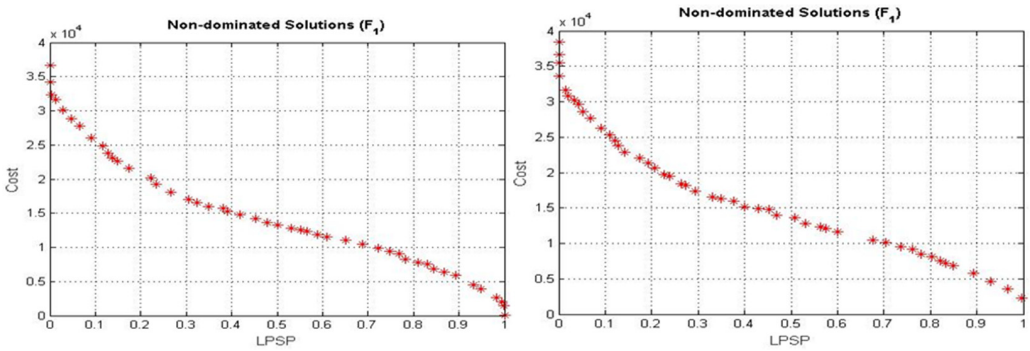

(a) (b)

Figure 8. (**a**) Cost versus LPSP graph employing NSGA-GWO Algorithm. (**b**) Cost versus LPSP graph employing NSGA II.

3.5. Cost Reduction with Loss of Power Supply Probability Relaxation

LPSP is the reliability factor in this study. The cost obtained by maintaining an LPSP of zero is defined as the most optimum cost. However, many researchers [36] consider any LPSP below 5%. Thus, Table 6 portrays the obtained reduced costs by allowing the LPSP to increase to about 9%, found by the best five independent runs of the proposed hybrid algorithm. It was observed from independent run 30 that if LPSP is allowed to increase to 1.23% from 0.37%, the cost reduces by 2.23%. If it is further increased to 4.70% from 1.23%, the cost decreases significantly by about 8.92%. If the LPSP keeps on increasing, the cost keeps on decreasing. However, it should be noted that an LPSP of 5% signifies that in a year of 8760 h, the load will remain unsupplied for 438 h, equivalent to more than 18 days in a year. The analysis is only shown for the best independent run out of 30 runs. However, the reduced obtained costs for the next four best simulations are also displayed. It is observed from Table 6 that various runs hit at various LPSPs and calculate the associated reduced costs of the components of the specified HRES. Therefore, LPSPs and the costs are all different in distinct runs.

Table 6. Changes in cost due to variation of LPSP.

Independent Run 30		Independent Run 2		Independent Run 1		Independent Run 7		Independent Run 27	
LPSP	**Cost ($)**	**LPSP**	**Cost ($)**	**LPSP**	**Cost ($)**	**LPSP**	**Cost ($)**	**LPSP**	**Cost ($)**
0%	32,797.48	0%	32,820.37	0%	32,820.37	0%	33,003.05	0%	33,205.67
0.37%	32,384.54	0.57%	32,857.76	2.15%	30,815.01	1.24%	32,225.76	0.64%	32,271.9
1.23%	31,675.48	1.99%	31,205.84	2.39%	30,561.09	3.11%	30,591.4	0.96%	31,959.67
2.96%	30,164.28	2.92%	30,181.42	4.36%	29,155.23	4.83%	28,820.55	1.83%	30,986.01
4.70%	28,847.06	3.72%	29,559.88	5.55%	28,531.56	8.17%	27,165.87	3.33%	29,806.89
6.46%	27,773.53	5.24%	28,735.21	7.08%	27,367.04	9.45%	26,335.23	4.84%	29,196.38
9.04%	26,015.12	7.08%	27,667.34	8.05%	26,713.54	10.33%	25,466.8	6.69%	27,984.08

3.6. Recommendations for Practical Implementation

The results obtained so far are, of course, theoretical, and the algorithm even considers fractions. However, a fractional number of WTs, PV panels, or batteries cannot be adopted for practical implementation. The algorithm is intentionally designed to take fractions as solutions because, unlike the problem at hand, many other problems often require/accept fractional values as solutions. Evaluating the algorithm at the fractional level gives a much more in-depth analysis. Thus, it is required to round up the values to the next integer and find the corresponding cost. Therefore, for practical implementation, the number of WTs, PV panels, and batteries are rounded up to the next integer for the three best-obtained results from the hybrid algorithm. The data obtained are displayed in Table 7. Although the cost now increases due to rounding up to the next integer value, this is equally applicable for other algorithms as well.

Table 7. Practical implementation.

Independent Run No.	30		2		7	
	Theoretical	**Practical**	**Theoretical**	**Practical**	**Theoretical**	**Practical**
N_{PV}	5.4244	6	4.5705	5	5.3778	6
N_{WG}	4.5978	5	4.9533	5	4.9795	5
N_{bat}	2×0.9312	2×1	2×0.8929	2×1	2×0.8996	2×1
β	19.5281	19.5281	1	1	3.0993	3.0993
h	38.6184	38.6184	35.2532	35.2532	33.4254	33.4254
Cost ($)	32,797.48	35,693.77	32,820.37	33,815.25	33,003.05	33,980.08

4. Conclusions

In this study, an evolutionary algorithm NSGA-II and a nature-inspired algorithm GWO were hybridized to optimize, keeping both LPSP and cost as decision variables, an HRES configuration consisting of PV, WT, and BS. The main objective was to find the minimum costs by varying the LPSP and providing the designer/company with all the potential solutions. The study's outcome signifies that the developed hybrid algorithm has a high probability of obtaining the global optimum solution. It also provides a much quicker convergence, a lower minimum cost, a lower mean, a normally distributed data set, and a higher standard deviation than the other two algorithms. From the presented case study, the optimum cost obtained among 30 independent runs was 32,797.48$ for the hybrid algorithm, whereas, for NSGA-II, it was 33,139.64$ and 36,512.70$ for MOPSO. Furthermore, the obtained mean values also signify the overall acceptability of the hybrid algorithm; 33,871.11$, 33,948.51$, and 69,637.78$ for the hybrid algorithm, NSGA-II, and MOPSO, respectively. Moreover, from the K-S and S-W tests, the asymptotic sigma values are 0.2 and 0.315, respectively, for the hybrid algorithm; for NSGA-II and MOPSO, in both the tests, the values are less than 0.05, signifying that the results obtained from the hybrid algorithm are in a normal distribution. The normal distribution data and a high standard

deviation imply that the hybrid algorithm not only explores larger search space but also provides many options for the designer/company.

It is essential to mention that the proposed HRES configuration is site-dependent. Before implementing any HRES configuration, the available energy sources of a particular site should be thoroughly evaluated, and only then can the choices of HRES components be made. However, the studied hybrid algorithm can be applied to any choice of HRES components. The authors firmly believe that this algorithm applies equally to other fields, provided necessary adjustments are made. Thus, this study is evidence of merging techniques to generate a hybrid multi-objective optimization algorithm that not only obtains a better result than a single method-based algorithm but can also outperform other algorithms for the sizing approaches in the field of HRES. The extension of this work may focus on incorporating real-time load along with weather uncertainties and adopting online optimization.

Author Contributions: All authors equally contributed to this paper. All authors have read and agreed to the published version of the manuscript.

Funding: This research received no external funding.

Data Availability Statement: The data that support the findings of this study are available from the corresponding author upon reasonable request.

Conflicts of Interest: The authors declare no conflict of interest.

References

1. Jacobson, M.Z.; Delucchi, M.A. Providing All Global Energy with Wind, Water, and Solar Power, Part I: Technologies, Energy Resources, Quantities and Areas of Infrastructure, and Materials. *Energy Policy* **2011**, *39*, 1154–1169. [CrossRef]
2. Nengroo, S.H.; Jin, H.; Lee, S. Management of Distributed Renewable Energy Resources with the Help of a Wireless Sensor Network. *Appl. Sci.* **2022**, *12*, 6908. [CrossRef]
3. Sawle, Y.; Gupta, S.C.; Bohre, A.K. Review of Hybrid Renewable Energy Systems with Comparative Analysis of Off-Grid Hybrid System. *Renew. Sustain. Energy Rev.* **2018**, *81*, 2217–2235. [CrossRef]
4. Deshmukh, M.; Deshmukh, S. Modeling of Hybrid Renewable Energy Systems. *Renew. Sustain. Energy Rev.* **2008**, *12*, 235–249. [CrossRef]
5. Auckland Council. Auckland's Electricity Network. Available online: http://www.aucklandcouncil.govt.nz/plans-projects-policies-reports-bylaws/our-plans-strategies/auckland-plan/development-strategy/Pages/aucklands-electricity-network.aspx (accessed on 15 December 2022).
6. Auckland Council. Decentralise Renewable Energy Solutions. Available online: http://www.aucklandcouncil.govt.nz/plans-projects-policies-reports-bylaws/our-plans-strategies/topic-based-plans-strategies/environmental-plans-strategies/aucklands-climate-plan/energy-industry/Pages/decentralise-renewable-energy-solutions.aspx (accessed on 15 December 2022).
7. Al-Ghussain, L.; Ahmed, H.; Haneef, F. Optimization of Hybrid PV-Wind System: Case Study Al-Tafilah Cement Factory, Jordan. *Sustain. Energy Technol. Assess.* **2018**, *30*, 24–36. [CrossRef]
8. Nengroo, S.H.; Ali, M.U.; Zafar, A.; Hussain, S.; Murtaza, T.; Alvi, M.J.; Raghavendra, K.; Kim, H.J. An Optimized Methodology for a Hybrid Photo-Voltaic and Energy Storage System Connected to a Low-Voltage Grid. *Electronics* **2019**, *8*, 176. [CrossRef]
9. Nengroo, S.H.; Lee, S.; Jin, H.; Har, D. Optimal Scheduling of Energy Storage for Power System with Capability of Sensing Short-Term Future PV Power Production. In Proceedings of the 11th International Conference on Power and Energy Systems (ICPES), Shanghai, China, 18–20 December 2021; IEEE: Piscataway, NJ, USA, 2021; pp. 172–177.
10. Rodrigues, E.; Godina, R.; Santos, S.F.; Bizuayehu, A.W.; Contreras, J.; Catalão, J. Energy Storage Systems Supporting Increased Penetration of Renewables in Islanded Systems. *Energy* **2014**, *75*, 265–280. [CrossRef]
11. Nelson, D.; Nehrir, M.; Wang, C. Unit Sizing and Cost Analysis of Stand-Alone Hybrid Wind/PV/Fuel Cell Power Generation Systems. *Renew. Energy* **2006**, *31*, 1641–1656. [CrossRef]
12. Hosseinalizadeh, R.; Shakouri, H.; Amalnick, M.S.; Taghipour, P. Economic Sizing of a Hybrid (PV–WT–FC) Renewable Energy System (HRES) for Stand-Alone Usages by an Optimization-Simulation Model: Case Study of Iran. *Renew. Sustain. Energy Rev.* **2016**, *54*, 139–150. [CrossRef]
13. Sheng, W.; Liu, K.; Meng, X.; Ye, X.; Liu, Y. Research and Practice on Typical Modes and Optimal Allocation Method for PV-Wind-ES in Microgrid. *Electr. Power Syst. Res.* **2015**, *120*, 242–255. [CrossRef]
14. Maleki, A.; Pourfayaz, F. Optimal Sizing of Autonomous Hybrid Photovoltaic/Wind/Battery Power System with LPSP Technology by Using Evolutionary Algorithms. *Sol. Energy* **2015**, *115*, 471–483. [CrossRef]
15. Khan, A.A.; Minai, A.F.; Pachauri, R.K.; Malik, H. Optimal Sizing, Control, and Management Strategies for Hybrid Renewable Energy Systems: A Comprehensive Review. *Energies* **2022**, *15*, 6249. [CrossRef]

16. Chowdhury, T.; Hasan, S.; Chowdhury, H.; Hasnat, A.; Rashedi, A.; Asyraf, M.R.M.; Hassan, M.Z.; Sait, S.M. Sizing of an Island Standalone Hybrid System Considering Economic and Environmental Parameters: A Case Study. *Energies* **2022**, *15*, 5940. [CrossRef]
17. Bhandari, B.; Poudel, S.R.; Lee, K.-T.; Ahn, S.-H. Mathematical Modeling of Hybrid Renewable Energy System: A Review on Small Hydro-Solar-Wind Power Generation. *Int. J. Precis. Eng. Manuf. Green Technol.* **2014**, *1*, 157–173. [CrossRef]
18. Smaoui, M.; Abdelkafi, A.; Krichen, L. Optimal Sizing of Stand-Alone Photovoltaic/Wind/Hydrogen Hybrid System Supplying a Desalination Unit. *Sol. Energy* **2015**, *120*, 263–276. [CrossRef]
19. Al-Falahi, M.D.; Jayasinghe, S.; Enshaei, H. A Review on Recent Size Optimization Methodologies for Standalone Solar and Wind Hybrid Renewable Energy System. *Energy Convers. Manag.* **2017**, *143*, 252–274. [CrossRef]
20. Hossain, M.; Mekhilef, S.; Olatomiwa, L. Performance Evaluation of a Stand-Alone PV-Wind-Diesel-Battery Hybrid System Feasible for a Large Resort Center in South China Sea, Malaysia. *Sustain. Cities Soc.* **2017**, *28*, 358–366. [CrossRef]
21. Li, C.; Ge, X.; Zheng, Y.; Xu, C.; Ren, Y.; Song, C.; Yang, C. Techno-Economic Feasibility Study of Autonomous Hybrid Wind/PV/Battery Power System for a Household in Urumqi, China. *Energy* **2013**, *55*, 263–272. [CrossRef]
22. Islam, M.R.; Akter, H.; Howlader, H.O.R.; Senjyu, T. Optimal Sizing and Techno-Economic Analysis of Grid-Independent Hybrid Energy System for Sustained Rural Electrification in Developing Countries: A Case Study in Bangladesh. *Energies* **2022**, *15*, 6381. [CrossRef]
23. Al-Badi, A.; Al Wahaibi, A.; Ahshan, R.; Malik, A. Techno-Economic Feasibility of a Solar-Wind-Fuel Cell Energy System in Duqm, Oman. *Energies* **2022**, *15*, 5379. [CrossRef]
24. Ahshan, R.; Hosseinzadeh, N.; Al-Badi, A.H. Economic Evaluation of a Remote Microgrid System for an Omani Island. *Int. J. Smart Grid Clean Energy* **2020**, *9*, 495–510. [CrossRef]
25. Anoune, K.; Laknizi, A.; Bouya, M.; Astito, A.; Abdellah, A.B. Sizing a PV-Wind Based Hybrid System Using Deterministic Approach. *Energy Convers. Manag.* **2018**, *169*, 137–148. [CrossRef]
26. Mazzeo, D.; Baglivo, C.; Matera, N.; Congedo, P.M.; Oliveti, G. A Novel Energy-Economic-Environmental Multi-Criteria Decision-Making in the Optimization of a Hybrid Renewable System. *Sustain. Cities Soc.* **2020**, *52*, 101780. [CrossRef]
27. Mazzeo, D.; Oliveti, G.; Baglivo, C.; Congedo, P.M. Energy Reliability-Constrained Method for the Multi-Objective Optimization of a Photovoltaic-Wind Hybrid System with Battery Storage. *Energy* **2018**, *156*, 688–708. [CrossRef]
28. Fathima, A.H.; Palanisamy, K. Optimization in Microgrids with Hybrid Energy Systems—A Review. *Renew. Sustain. Energy Rev.* **2015**, *45*, 431–446. [CrossRef]
29. Clarke, D.P.; Al-Abdeli, Y.M.; Kothapalli, G. Multi-Objective Optimisation of Renewable Hybrid Energy Systems with Desalination. *Energy* **2015**, *88*, 457–468. [CrossRef]
30. Tozzi, P., Jr.; Jo, J.H. A Comparative Analysis of Renewable Energy Simulation Tools: Performance Simulation Model vs. System Optimization. *Renew. Sustain. Energy Rev.* **2017**, *80*, 390–398. [CrossRef]
31. Zhang, J.; Tang, Q.; Chen, Y.; Lin, S. A Hybrid Particle Swarm Optimization with Small Population Size to Solve the Optimal Short-Term Hydro-Thermal Unit Commitment Problem. *Energy* **2016**, *109*, 765–780. [CrossRef]
32. Koutroulis, E.; Kolokotsa, D.; Potirakis, A.; Kalaitzakis, K. Methodology for Optimal Sizing of Stand-Alone Photovoltaic/Wind-Generator Systems Using Genetic Algorithms. *Sol. Energy* **2006**, *80*, 1072–1088. [CrossRef]
33. Amer, M.; Namaane, A.; M'sirdi, N. Optimization of Hybrid Renewable Energy Systems (HRES) Using PSO for Cost Reduction. *Energy Procedia* **2013**, *42*, 318–327. [CrossRef]
34. Bukar, A.L.; Tan, C.W.; Lau, K.Y. Optimal Sizing of an Autonomous Photovoltaic/Wind/Battery/Diesel Generator Microgrid Using Grasshopper Optimization Algorithm. *Sol. Energy* **2019**, *188*, 685–696. [CrossRef]
35. Fadaee, M.; Radzi, M. Multi-Objective Optimization of a Stand-Alone Hybrid Renewable Energy System by Using Evolutionary Algorithms: A Review. *Renew. Sustain. Energy Rev.* **2012**, *16*, 3364–3369. [CrossRef]
36. Bilal, B.O.; Sambou, V.; Ndiaye, P.; Kébé, C.; Ndongo, M. Multi-Objective Design of PV-Wind-Batteries Hybrid Systems by Minimizing the Annualized Cost System and the Loss of Power Supply Probability (LPSP). In Proceedings of the IEEE International Conference on Industrial Technology (ICIT), Cape Town, South Africa, 25–28 February 2013; pp. 861–868.
37. Kamjoo, A.; Maheri, A.; Dizqah, A.M.; Putrus, G.A. Multi-Objective Design under Uncertainties of Hybrid Renewable Energy System Using NSGA-II and Chance Constrained Programming. *Int. J. Electr. Power Energy Syst.* **2016**, *74*, 187–194. [CrossRef]
38. N'guessan, S.A.; Agbli, K.S.; Fofana, S.; Hissel, D. Optimal Sizing of a Wind, Fuel Cell, Electrolyzer, Battery and Supercapacitor System for off-Grid Applications. *Int. J. Hydrogen Energy* **2020**, *45*, 5512–5525.
39. Ghorbani, N.; Kasaeian, A.; Toopshekan, A.; Bahrami, L.; Maghami, A. Optimizing a Hybrid Wind-PV-Battery System Using GA-PSO and MOPSO for Reducing Cost and Increasing Reliability. *Energy* **2018**, *154*, 581–591. [CrossRef]
40. Mahmoud, F.S.; Diab, A.A.Z.; Ali, Z.M.; El-Sayed, A.-H.M.; Alquthami, T.; Ahmed, M.; Ramadan, H.A. Optimal Sizing of Smart Hybrid Renewable Energy System Using Different Optimization Algorithms. *Energy Rep.* **2022**, *8*, 4935–4956. [CrossRef]
41. Kaur, R.; Krishnasamy, V.; Kandasamy, N.K.; Kumar, S. Discrete Multiobjective Grey Wolf Algorithm Based Optimal Sizing and Sensitivity Analysis of PV-Wind-Battery System for Rural Telecom Towers. *IEEE Syst. J.* **2020**, *14*, 729–737. [CrossRef]
42. Deb, K.; Agrawal, S.; Pratap, A.; Meyarivan, T. A Fast Elitist Non-Dominated Sorting Genetic Algorithm for Multi-Objective Optimization: NSGA-II. In International Conference on Parallel Problem Solving from Nature, Proceedings of the 6th International Conference, Paris, France, 18–20 September 2020; Springer: Berlin/Heidelberg, Germany, 2020; pp. 849–858.
43. Mirjalili, S.; Mirjalili, S.M.; Lewis, A. Grey Wolf Optimizer. *Adv. Eng. Softw.* **2014**, *69*, 46–61. [CrossRef]

44. Tito, M.R.; Lie, T.T.; Anderson, T. Sizing Optimization of Wind-Photovoltaic Hybrid Energy Systems Under Transient Load. *Int. J. Power Energy Syst.* **2013**, *33*, 168–174. [CrossRef]
45. The Electricity Authority, 2014. Available online: https://www.ea.govt.nz/dmsdocument/4755 (accessed on 4 November 2022).
46. Weather Data Center. Available online: https://www.ashrae.org/technical-resources/bookstore/weather-data-center (accessed on 23 November 2022).
47. Chedid, R.; Akiki, H.; Rahman, S. A Decision Support Technique for the Design of Hybrid Solar-Wind Power Systems. *Int. Trans. Energy Convers.* **1998**, *13*, 76–83. [CrossRef]
48. Mukund, R.P. *Wind and Solar Power Systems*; CRC Press: Boca Raton, FL, USA, 1999.
49. Borowy, B.S.; Salameh, Z.M. Methodology for Optimally Sizing the Combination of a Battery Bank and PV Array in a Wind/PV Hybrid System. *IEEE Trans. Energy Convers.* **1996**, *11*, 367–375. [CrossRef]
50. Ahshan, R. Potential and Economic Analysis of Solar-to-Hydrogen Production in the Sultanate of Oman. *Sustainability* **2021**, *13*, 9516. [CrossRef]
51. Yang, H.; Zhou, W.; Lu, L.; Fang, Z. Optimal Sizing Method for Stand-Alone Hybrid Solar–Wind System with LPSP Technology by Using Genetic Algorithm. *Sol. Energy* **2008**, *82*, 354–367. [CrossRef]
52. Guasch, D.; Silvestre, S. Dynamic Battery Model for Photovoltaic Applications. *Prog. Photovolt. Res. Appl.* **2003**, *11*, 193–206. [CrossRef]
53. Yang, H.; Lu, L. Study of Typical Meteorological Years and Their Effect on Building Energy and Renewable Energy Simulations. *ASHRAE Trans.* **2004**, *110*, 424.
54. Peng, W.; Zhang, Q.; Li, H. Comparison between MOEA/D and NSGA-II on the Multi-Objective Travelling Salesman Problem. In *Multi-Objective Memetic Algorithms*; Springer: Berlin/Heidelberg, Germany, 2009; pp. 309–324.
55. Higham, D.J.; Higham, N.J. *MATLAB Guide 2016*, 3rd ed.; SIAM-Society for Industrial and Applied Mathematics: Philadelphia, PA, USA, 2016; ISBN 978-1-61197-465-2.
56. SPSS Inc. *SPSS-X User's Guide*, 3rd ed.; SPSS Europe: Chicago, IL, USA; Gorinchem, The Netherlands, 1988; ISBN 978-0-918469-51-9.